INCREASING THE ROBUSTNESS OF AN INVERSE STAMPING ALGORITHM

JAROMIR KASPAR[1], PETR BERNARDIN[1], VACLAVA LASOVA[1]

[1]University of West Bohemia in Pilsen, Faculty of Mechanical Engineering, Department of Machine Design

Inverse stamping is a useful tool in engineering. It can be used to find the initial blank shape of stamped parts. It is also useful for quick and easy analysis of a forming process and its impact on the design of a component. Algorithms for inverse stamping are commonly available, but in some situations these algorithms can collapse or may provide confusing results. This article describes improvements to a newly designed inverse stamping algorithm which lead to an increase in its robustness.

KEYWORDS

Inverse stamping, robustness, finite element method, forming, metal sheet.

1 INTRODUCTION

Advantage of the inverse stamping method is short calculation time and simple user interface. Compared with standard numerical simulation of forming, it needs less inputs. The models of forming tools are not required and no forming process parameters are needed as well. Therefore, it is not possible to perform standard numerical simulation of forming in many situations, because all needed inputs are not yet available. The inverse stamping is the only one alternative in such cases.

Inverse stamping [Yu 2005, Mackerle 2004] is a simplified method to analyse the forming process of metal sheet bodies based on the inverse finite element approach [Lan 2005, Huang 2006]. Some assumptions are made. Especially, the inverse stamping algorithm assumes that all the forming operations are done in one step. Real forming processes are usually split into a sequence of forming operations. This difference could lead to problems in some situations. An example of a problematic forming process is described in Figure 1 - Figure 3. The body to be formed has three parts. Part A is fixed in space during the whole forming process. Part B reaches its final position by rotation about its x-axis, see operation 1 in Figure 2. Part C is rotated about the x-axis and then about the z-axis, see Operation 1 in Figure 2, and operation 2 in Figure 3. Part C can pose a problem for the inverse stamping algorithm due to two consecutive rotations around two different axes.
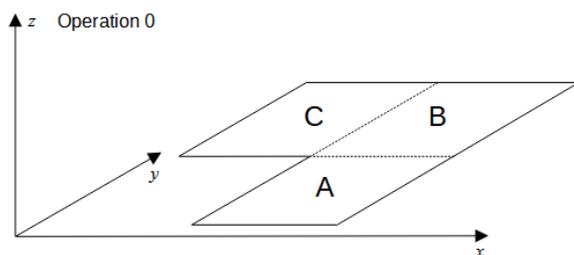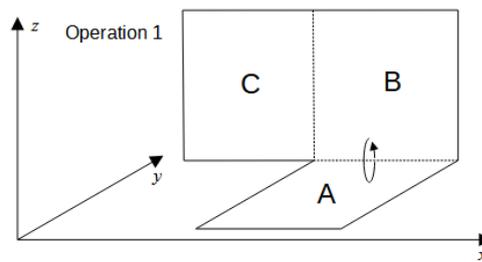

Figure 1. Forming step 1 – Operation 0
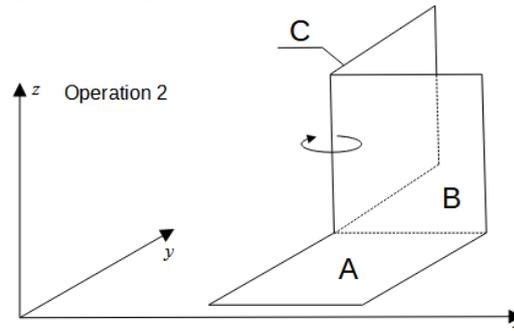

Figure 2. Forming step 2 – Operation 1

Figure 3. Forming step 3 – Operation 2

2 INVERSE STAMPING ALGORITHM

The traditional inverse finite element method with unfolding technique has three main steps:

1. The three-dimensional part is projected onto a flat plane, i.e. initial guess of the two-dimensional blank shape is made.
2. Two-dimensional finite element method is used for iterative improvement of the blank shape.
3. Important quantities are evaluated.

It was found that some existing algorithms using the inverse stamping method are not suitable or applicable for some parts with certain shapes (the calculation does not converge or collapses). Therefore, it was necessary to design a new algorithm for a simplified calculation of residual stress and residual deformation in those parts. This new algorithm uses a new reduction method (First step - see above) for unfolding the part. The development of this algorithm and the unique reduction method was described and published in [Kaspar 2021]. The second step has the following sub-steps [Azizi 2008], [Farahani 2014]:

a. Each element is unfolded
b. Nodal displacements $\{Δu_e\}$ of each element are calculated as the difference between unfolded and projected nodal coordinates. Nodal forces are calculated.
c. Global stiffness matrix $[K]$ and external forces vector $\{F\}$ are assembled. Increment of nodal displacements $\{Δu\}$ are calculated as a solution of linear equations system $[K]\{Δu\}=[F]$
d. Nodal coordinates are updated by adding $\{Δu\}$
e. Material properties are updated
f. After the convergence criterion is fulfilled, the second step is stopped. Otherwise, the algorithm goes to sub-step b.

Sub-step a. is the key point of the procedure presented in this article. In [Shirin 2014] the unfolding of the element is described as the rotation of an element about angle $α$, equation (1), where $\{n\}$ denotes element normal vector and $\{k\}$ denotes projection plane normal vector.

$$\alpha = arccos(\{n\}\{k\}) \tag{1}$$

Rotational matrix is given by equation (2).

$$[R] =$$
$$\begin{bmatrix} m_1^2\mu + cos\alpha & m_1m_2\mu - m_3sin\alpha & m_1m_3\mu + m_2sin\alpha \\ m_1m_2\mu + m_3sin\alpha & m_2^2\mu + cos\alpha & m_2m_3\mu - m_1sin\alpha \\ m_1m_3\mu - m_2sin\alpha & m_2m_3\mu + m_1sin\alpha & m_3^2\mu + cos\alpha \end{bmatrix} \tag{2}$$

Rotation direction vector is given by equation (4) and angle μ is given by equation (3).

$$\mu = 1 - cos\alpha \tag{3}$$

$$\{m_1 \quad m_2 \quad m_3\}^T = \frac{1}{\|\{n\}\times\{k\}\|}\{n\} \times \{k\} \tag{4}$$

The triangular element related to part C with nodes n_1, n_2, n_3 and the unfolded element with nodes $n_{1,u}$, $n_{2,u}$, $n_{3,u}$ is shown in Figure 4. Nodal positions $n_{1,u}$, $n_{2,u}$, $n_{3,u}$ are obtained using equations (1)-(4).
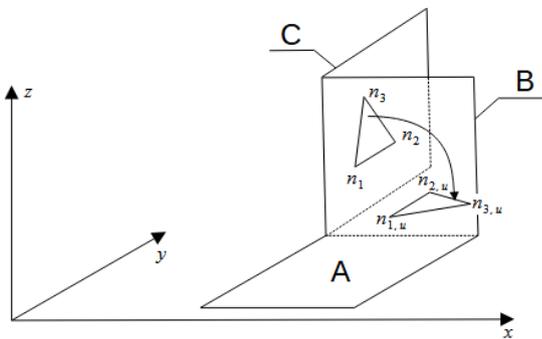

Figure 4. Element unfolding

The same element related to the initial blank shape is shown in Figure 5.
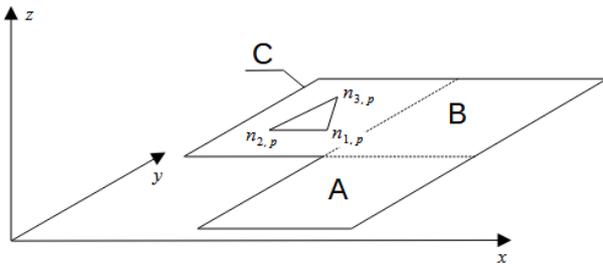

Figure 5. Initial blank shape element

From the comparison of the unfolded element and the initial blank shape element, Figure 6, it is clear that the unfolded element is rotated about 90° compared to the initial blank shape element.
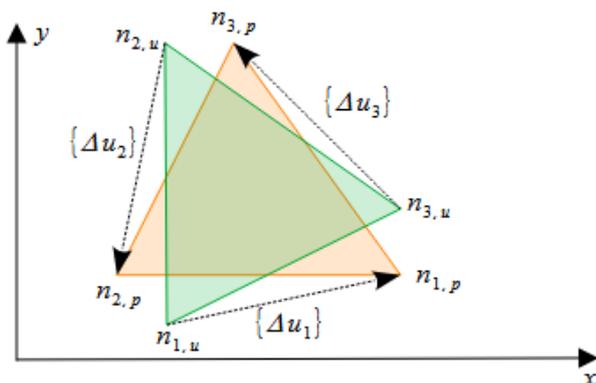

Figure 6. Element comparison

Force vector $\{F_e\}$ acting on single element is given by equation (5), where $[K_e]$ denotes element stiffness matrix and $\{\Delta u_e\}$ is vector of element nodes displacements.

$$\{F_e\} = [K_e]\{\Delta u_e\} \tag{5}$$

Displacements and external forces are calculated for each element and vectors $\{F_e\}$ are arranged into common force vector $\{F\}$ in sub-step b. Distortion of part C occurs in sub-step c. and d., when nodal displacements are calculated and nodal positions are updated. Force vector $\{F\}$ tends to rotate elements of part C, which cause its distortion. This is shown in Figure 7 and Figure 8, with flat shapes after iterations 1-4. The distortion of part C is clearly visible.
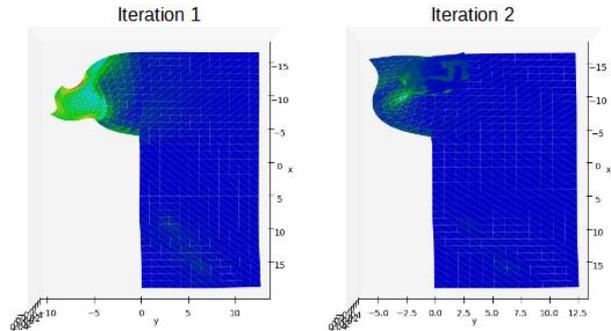

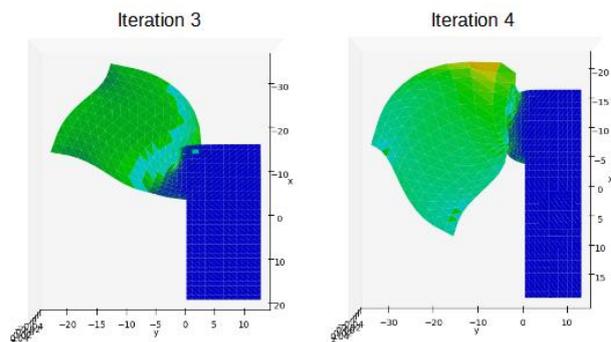**Figure 7.** Improvement iteration 1 and 2

Figure 8. Improvement iteration 3 and 4

3 PROPOSED SOLUTION

It is common practice in the finite element method to use corotational theory when a large deflection problem is solved. The idea of this theory is to decompose the element configuration into a rigid part and a deformation component. This approach is also applicable to the inverse stamping method.

Figure 9 shows the rigid motion of the unfolded element. The green element with nodes $n_{1,u}$, $n_{2,u}$, $n_{3,u}$ is the unfolded element. The blue element with nodes $n'_{1,u}$, $n'_{2,u}$, $n'_{3,u}$ is the unfolded element after the rigid motion is removed. The orange element with nodes $n_{1,p}$, $n_{2,p}$, $n_{3,p}$ is the projected element.
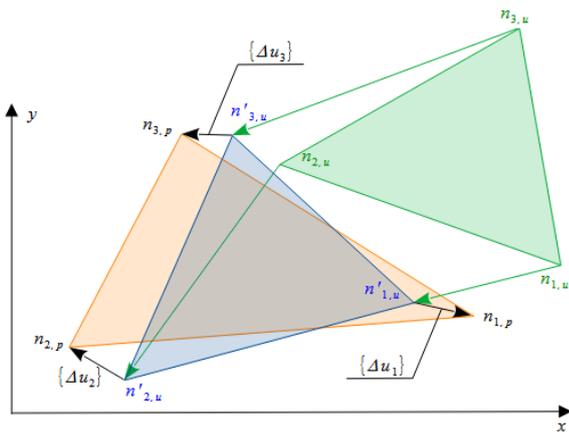
Figure 9. Rigid motion of unfolded element

[Mostafa 2014] proposes a procedure for finding the configuration of the element which minimizes nodal displacements $\{\Delta u_i\}$, i=1, 2, 3. This method was added to the second step of the inverse stamping algorithm.

The sub-steps of the second stage in our approach are:

    a. Each element is unfolded.

    b. Iteration number is initialized to $j=0$.

    c. Rigid motions of unfolded elements are removed. Nodal positions $n'_{i,u}$ of unfolded elements are stored.

    d. Nodal displacements $\{\Delta u_i\}$ of each element are calculated as the difference between nodal positions $n'_{i,u}$ and projected nodal positions $n_{i,p}$. Nodal forces are calculated based on nodal displacements.

    e. Global stiffness matrix $[K]$ and external forces vector $\{F\}$ are assembled. Increment of nodal displacements $\{\Delta u\}$ is calculated as a solution of linear equations system $[K]\{\Delta u\} = [F]$.

    f. Projected nodal coordinates are updated by adding $\{\Delta u\}$.

    g. Material properties are updated.

    h. Iteration number is increased to $j=j+1$

    i. After the convergence criterion is fulfilled, the second step is stopped. Otherwise, if $j<10$, then the algorithm goes to sub-step c., or else the algorithm goes to sub-step d.

The positions of the unfolded element are updated only if j is lower than ten. The purpose of this condition is to accelerate the solution process. If the unfolded element positions are updated in every iteration then the nodal forces calculated based on $\{\Delta u_i\}$ could oscillate and it is difficult to achieve convergence. After reaching ten iterations, the changes of nodal positions $n'_{i,u}$ are small and can be neglected. Figure 10 and Figure 11 shows the first four improvement iterations using our new approach. There is no distortion of body part C (compared to Figure 7 and Figure 8). Increased element deformation is noticeable around nodes where boundary conditions were applied. Those deformations vanish in the next iterations.
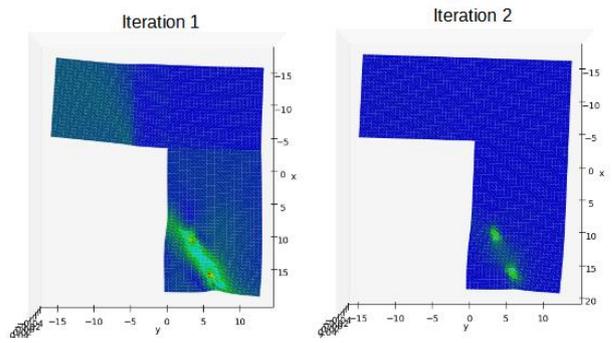

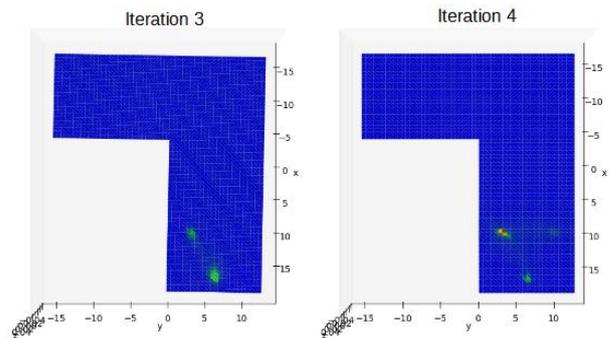Figure 10. Improvement iterations of our algorithm

Figure 11. Improvement iterations of our algorithm

In our algorithm, the unfolded elements are oriented based on the projected elements. This procedure is successful if the quality of the initial projection is good enough. Therefore, the first step of the inverse stamping method was solved using the algorithm described in [Kaspar 2021].

4 RESULTS AND DISCUSSION

Here we compare the inverse stamping algorithms and classical numerical forming simulation. Three different inverse stamping algorithms were used – original inverse stamping algorithm, newly proposed inverse stamping algorithm and commercial software Siemens NX Analyze Formability One-Step (NX AFSO).

Two sheet metal bodies were used. The first body (body B1) is similar to the body in Figure 3. Figure 12 shows equivalent plastic strain as a result of numerical simulation.
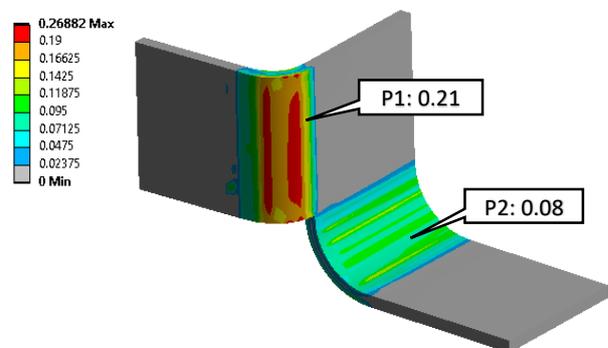

Figure 12. Equivalent plastic strain based on numerical simulation, body B1

Figure 13 shows equivalent plastic strain as a result of the new inverse stamping algorithm. The blue line in Figure 13 represents the initial blank shape. Two points, P1 and P2, were chosen as reference.

If the original inverse stamping algorithm is used then the solution process fails because of the distortion shown in Figure 8.
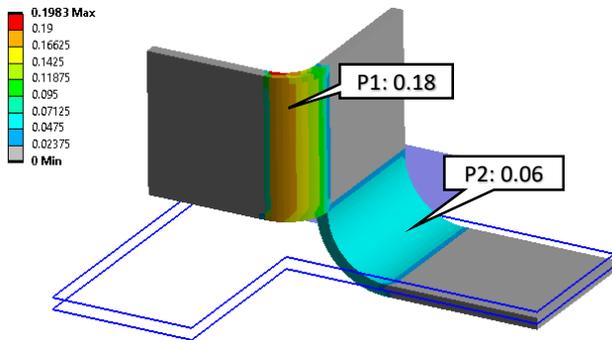

Figure 13. Equivalent plastic strain based on our new algorithm, body B1

Similar comparisons were made for body B2 which is shown in Figure 14. Figure 14 shows equivalent plastic strain as a result of numerical simulation. P3 and P4 were chosen as reference points.
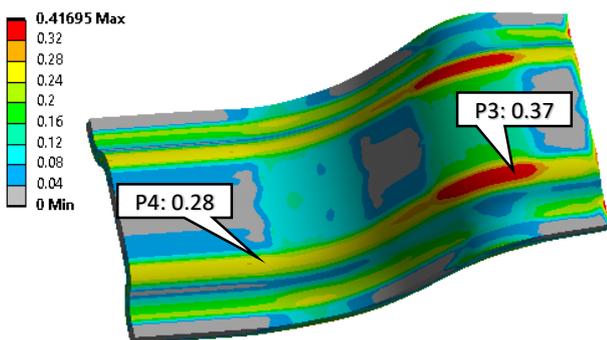

Figure 14. Equivalent plastic strain based on numerical simulation, body B2

Figure 15 shows equivalent plastic strain as a result of the new algorithm.
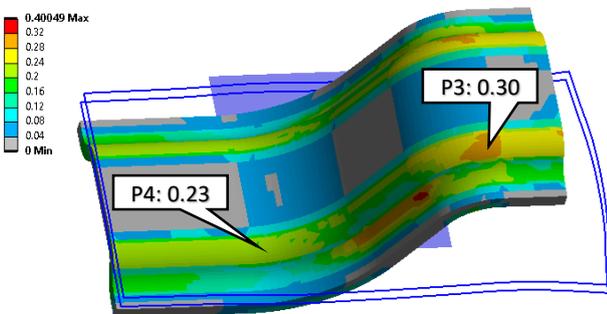

Figure 15. Equivalent plastic strain based on the new algorithm, body B2

The original algorithm worked well when body B2 was analysed. Equivalent plastic strain based on the original algorithm is shown in Figure 16.
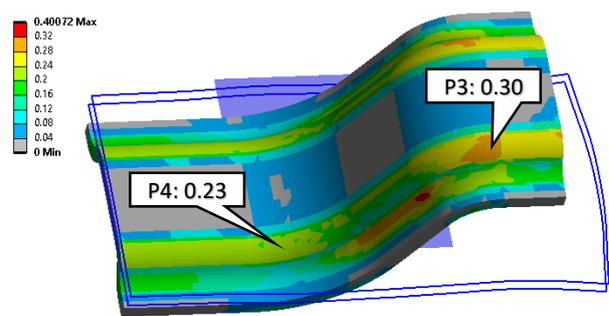

Figure 16. Equivalent plastic strain based on original algorithm, body B2

Both inverse stamping algorithms provide similar results for body B2. Also, the number of iterations is the same for the original algorithm and the new one. It should be noted that using our new algorithm could lead to a higher number of iterations in some cases. Some differences in equivalent plastic strain distribution are noticed if inverse stamping and numerical simulation are compared. This is caused by simplifications typical for inverse stamping. Numerical simulation of body B1 and body B2 included two consecutive forming operations. The inverse stamping algorithm assumes that all forming operations are done at once. Also, other simplifications and assumptions have to be made when an inverse stamping algorithm is created. Body B1 showed that the original algorithm failed and did not provide any results. Our solution increases the robustness of the inverse stamping algorithm and can be used for a new class of bodies. The resulting equivalent plastic strain of Body B1 is shown in Table 1.

Body	Point	Algorithm	Eqv. Plast. Strain [-]	No. of iterations
B1	P1	Proposed	0.18	13
		Original	failed	failed
		Simulation	0.21	-
		NX AFOS	0.23	-
	P2	Proposed	0.06	13
		Original	failed	failed
		Simulation	0.08	-
		NX AFOS	0.11	-

Table 1. Results summary of Body B1

The resulting equivalent plastic strain of Body B2 is shown in Table 2.

Body	Point	Algorithm	Eqv. Plast. Strain [-]	No. of iterations
B2	P3	Proposed	0.30	11
		Original	0.30	11
		Simulation	0.37	-
		NX AFOS	0.35	-
	P4	Proposed	0.23	11
		Original	0.23	11
		Simulation	0.28	-
		NX AFOS	0.25	-

Table 2. Results summary of Body B2

No distortions were observed when commercial software NX AFSO was used for analysis of body B1 and B2. Number of internal iterations done by this software is unknown. Probably, NX AFSO uses similar approach which is presented in this paper. Nevertheless, description of its algorithm wasn't published.

5 CONCLUSIONS

Inverse stamping is a useful tool for quick and easy analysis of forming effects. Its ease of use depends on the algorithm's reliability and robustness. It was shown that the original inverse stamping method could fail in some situations and we designed a solution for this problem. The improved algorithm provides higher robustness and eliminates the deficiencies of the previous algorithm. The number of improvement iterations of the new algorithm is comparable with the number of improvement iterations of the original algorithm, i.e. the impact on the method's calculation time is low.

The new algorithm was demonstrated here on the example of two bodies. Nevertheless, the authors tested this new algorithm on more than ten bodies of different shapes and no problems with distortion were observed.

REFERENCES

[Azizi 2008] Azizi, R. and Assempour, A. Applications of linear inverse finite element method in prediction of the optimum blank in sheet metal forming. Materials and Design, December 2008, Volume 29, Issue 10, pp 1965-1972, ISSN 0264-1275.

[Farahani 2014] Farahani, M.K. et al. Development of an inverse finite element method with an initial guess of linear unfolding. Finite Elements in Analysis and Design, February 2014, Volume 79, pp 1-8, ISSN 0168-874X.

[Huang 2006] Huang, Y. et al A new approach to solve key issues in multi-step inverse finite-element method in sheet metal stamping. In International Journal of Mechanical Sciences (Vol. 48, Issue 6, pp. 591–600). Elsevier BV. https://doi.org/10.1016/j.ijmecsci.2006.01.007

[Kaspar 2021] Kaspar, J. et al. Dimension Reduction Using the Inverse Stamping Method. MM Science Journal, October 2021, pp 4810-4817, ISSN 1805-0476.

[Lan 2005] Lan, J. et al Inverse finite element approach and its application in sheet metal forming. . In Journal of Materials Processing Technology (Vol. 170, Issue 3, pp. 624–631). Elsevier BV. https://doi.org/10.1016/j.jmatprotec.2005.06.043

[Mackerle 2004] Mackerle, J. Finite element analyses and simulations of sheet metal forming processes. In Engineering Computations (Vol. 21, Issue 8, pp. 891–940). Emerald. https://doi.org/10.1108/02644400410554371

[Mostafa 2014] Mostafa, M. and Sivaselvan, M.V. On best-fit corotated frames for 3D continuum finite elements, International Journal for Numerical Methods in Engineering, January 2014, Volume 98, Issue 2, pp 105-130, ISSN 1097-0207.

[Shirin 2014] Shirin, M.B. and Assempour, A. Some improvements on the unfolding inverse finite element method for simulation of deep drawing process. The International Journal of Advanced Manufacturing Technology, February 2014, Volume 72, pp 447–456, ISSN 1433-3015.

[Yu 2005] Yu, M. Sensitivity Analysis of the Sheet Metal Stamping Processes Based on Inverse Finite Element Modeling and Monte Carlo Simulation. In AIP Conference Proceedings. NUMISHEET 2005: Proceedings of the 6th International Conference and Workshop on Numerical Simulation of 3D Sheet Metal Forming Process. AIP. https://doi.org/10.1063/1.2011322

CONTACTS:

Ing. Jaromir Kaspar
University of West Bohemia in Pilsen, Faculty of Mechanical Engineering, Department of Machine Design
Univerzitni 22, 306 14 Pilsen, Czech Republic,
tel. +420 778 203 443, e-mail: jkaspar@kks.zcu.cz

Ing. Petr Bernardin, Ph.D.
University of West Bohemia in Pilsen, RTI - Regional Technological Institute, Faculty of Mechanical Engineering
Univerzitni 22, 306 14 Pilsen, Czech Republic,
tel.: +420 377 63 8263, e-mail: berny@kks.zcu.cz

prof. Ing. Vaclava Lasova, Ph.D.
University of West Bohemia in Pilsen, RTI - Regional Technological Institute, Faculty of Mechanical Engineering
Univerzitni 22, 306 14 Pilsen, Czech Republic,
tel.: +420 377 63 8264, e-mail: lasova@rti.zcu.cz